Thermal and Rheological Characteristics of Biobased Carbon Fiber Precursor Derived from Low Molecular Weight Organosolv Lignin

Azam Oroumei,[†,‡] Bronwyn Fox,[†,‡] and Minoo Naebe*[,†,‡]

[†]Institute for Frontier Materials, Deakin University, Geelong, Victoria 3216, Australia
[‡]Carbon Nexus, Deakin University, Geelong, Victoria 3216, Australia

S *Supporting Information*

ABSTRACT: In the present work, electrospinnability as well as thermal, rheological, and morphological characteristics of low molecular weight hardwood organosolv lignin, as a potential precursor for carbon fiber, was investigated. Submicromter biobased fibers were electrospun from a wide range of polymer solutions with different ratios of organosolv lignin to polyacrylonitrile (PAN). Rheological studies were conducted by measuring viscosity, surface tension, and electrical conductivity of hybrid polymer solutions, and used to correlate electrospinning behavior of solutions with the morphology of the resultant electrospun composite fibers. Using scanning electron microscopy (SEM) images, the solutions that led to the formation of bead-free uniform fibers were found. Differential scanning calorimetry (DSC) analysis revealed that lignin-based fibers enjoy higher decomposition temperatures than that of pure PAN. Thermal stability of the lignin-based fibers was investigated by thermogravimetric analysis (TGA) indicating a high carbon yield of above 50% at 600 °C, which is highly crucial in the production of low-cost carbon fiber. It was also observed that organosolv lignin synergistically affects thermal decomposition of composite fibers. A significant lower activation energy was found for the pyrolysis of lignin-derived electrospun fibers compared to that of pure PAN.

KEYWORDS: *Carbon fiber, Lignin, Biopolymer, Synergistic effect, Kinetics, Electrospinning*

INTRODUCTION

In recent decades, due to the increasing demand for biorenewable and eco-friendly resources, biopolymers have drawn considerable attention. This is, in particular, a result of rising environmental concerns surrounding polymers derived from nonrenewable sources such as fossil fuels, oil, and coal.[1−3] Furthermore, nonbiodegradability or poor biodegradability of most petrochemicals has intensified environmental concerns over continuing their consumption.[4] On the other hand, low process cost as well as low energy requirements are some of the interesting features of renewable biomaterials.[5]

In general, biopolymers are classified into natural and synthetic polymers.[6] Lignin is one of the natural biopolymers that exists in the cell wall of plants, and is basically a byproduct of wood pulping. Lignin is the second most abundant natural polymer after cellulose, and is one of the most important renewable resources on earth.[7] A range of industrial applications such as adsorbents,[8] adhesives,[9] dispersants and binders,[10] and soil preservation[11] has already been demonstrated for lignin.

Production of fibers from lignin has recently attracted the attention of many researchers in order to further implement this biopolymer for broader commercial industrial applications. One of the most promising applications of lignin fibers is the use of them as an environmentally sustainable precursor in the production of carbon fibers[12] that also will reduce the manufacturing costs of carbon fiber.[13] The abundance of aromatic components in the molecular structure of lignin makes it a good candidate for a carbon fiber precursor.[14] Although there are some processing challenges in producing fibers from lignin, some researchers have blended lignin with other polymers to facilitate the fiber production process, and as such, blending lignin with polymers has been investigated as a convenient and inexpensive approach to produce fibers. The literature shows several studies reporting melt spinning of various polymer blends (polyblends) with lignin.[13] Nonetheless, the resultant carbon fibers are fairly weak in comparison with those derived from petroleum-based precursors.[15]

Electrospinning, as another method of fiber production, has also been reported to produce submicrometer lignin fibers with high surface area and multifunctional characteristics,[16,17] by which the resultant carbon fibers can be applied in a wider range of applications like energy storage, adsorption/separation, and composites.[18]

As far as the production of carbon fibers is concerned, the purity of the precursor is a critical factor to potentially achieve a larger carbon yield.[19] There are a variety of lignins available in the market, depending on the isolation approach when lignin is being extracted from pulp. The major type of lignin is known as kraft lignin, which can be generated from the conventional kraft

pulping process.[14,20] However, kraft lignin contains inorganic impurities like ashes and salts.[21] In contrast, organosolv lignin, as another type of lignin, enjoys higher purity and is known as a sulfur-free lignin with low ash and carbohydrate content.[12,19] Apart from higher purity of organosolv lignin, this should be pointed out that it is the byproduct of solvent pulping process which is known as an environmentally friendly pulping technique.[10] Moreover, it has been reported that hardwood lignin shows good fiber spinnability,[3] in contrast with softwood lignin with poor processability in spinning.[22] According to Kadla et al.[23] hardwood kraft lignin and Alcell lignin are appropriate for conversion to carbon fibers with generally acceptable mechanical properties. While there are several reports in the literature on electrospinning of kraft lignin (Table 1), only a few studies have been conducted on electrospun organosolv lignin nanofibers.

Table 1. Summary of Literature Reports on Kraft Lignin-based Electrospun Nanofibers

type of lignin	auxiliary polymer	year	reference
softwood kraft lignin	poly(vinyl alcohol) (PVA)	2012	24
softwood kraft lignin	poly(ethylene oxide) (PEO)	2013	25
softwood kraft lignin	poly(vinyl alcohol) (PVA)	2014	14
kraft lignin	polyacrylonitrile (PAN)	2013	26
sodium carbonate lignin	poly(ethylene oxide) (PEO)	2012	27
kraft lignin	poly(ethylene oxide) (PEO)	2013	28
softwood kraft lignin	poly(ethylene oxide) (PEO)	2012	29
kraft lignin	polyacrylonitrile (PAN)	2011	30
softwood kraft lignin	poly(ethylene oxide) (PEO)	2013	31
alkali kraft lignin	polyacrylonitrile (PAN)	2013	32
alkali kraft lignin	polyacrylonitrile (PAN)	2014	33
sodium carbonate lignin	chitosan/poly(ethylene oxide) (PEO)	2014	34
kraft lignin	Poly(ethylene oxide) (PEO)	2015	35

Dallmeyer et al.[16] examined seven different technical lignins, including organosolv lignin, and found that electrospinning of lignin is possible if poly(ethylene oxide) (PEO) is used in the polymer blend. However, a precaution had be taken not to use more than 5% PEO in the blend, because higher amount of PEO caused fusion of lignin/PEO fibers together in pyrolysis, as a result of low glass transition of PEO. In another study, organosolv lignin (Alcell) was electrospun by Lallave et al.,[21] who dissolved Alcell lignin in ethanol and produced solid and hollow fibers through coaxial and triaxial electrospinning configurations. They reported fiber formation from Alcell lignin without addition of any other polymer; however, owing to the volatile nature of ethanol as solvent, a coaxial spinneret was used to compensate the amount of solvent loss, in which excess amount of ethanol was injected as a sheath around polymer. Wang et al.[36] prepared electrospun polyblend organosolv (Alcell) lignin nanofibers from hybrid solution of poly(ethylene oxide) and Alcell lignin for the production of carbon nanofibers. As per their studies on electrochemical properties of Alcell lignin-derived carbon nanofibrous mats, the resultant carbon nanofibers showed good cyclic stability suitable for energy storage applications such as lithium-ion batteries. Schreiber et al.[37] investigated the effect of iodine treatment on morphological retention of electrospun organosolv lignin/cellulose acetate fibers, and found that iodine

treated electrospun fibers can retain their original morphology during the heating process.

To the best of our knowledge, there is no report in the literature investigating the electrospinning of the fairly pure type of lignin, organosolv lignin, with PAN. The current work aims to investigate the electrospinning of hardwood organosolv lignin through the addition of a minimum amount of polacrylonitrile (PAN) as the most common and widely used precursor of carbon fiber. To further explore the structure−property relationships of the resultant as-spun lignin-based fibers, precise attention is drawn to the correlation between rheology of electrospinning solutions and pyrolysis and morphological properties of fibers.

■ EXPERIMENTAL SECTION

Materials. Water insoluble hardwood HP-L Organosolv Lignin powder (Lignol Lignin) with molecular weights of M_w ~1900 g/mol and M_n ~900 g/mol was obtained from Lignol Innovations Ltd., Canada. Polyacrylonitrile (PAN) with an average molecular weight of M_w 150 000 g/mol (typical, CAS Number 25014-41-9) was purchased from Sigma-Aldrich. N,N-Dimethylformamide (DMF), as a solvent (product number 103053), was obtained from Merck KGaA, Germany. All chemicals were used as received without further purification.

Preparation of Electrospun Nanofibers. Electrospinning solutions containing given amounts of lignin and PAN with an overall concentrations ranging from 18 to 55 wt % (relative to the weight of solvent) were prepared using the respective amount of DMF as the solvent. PAN was first dissolved in DMF under constant stirring for 2 h until a clear and homogeneous solution was obtained. Subsequently, the defined amount of lignin powder was added to the solution and stirring was continued for 24 h. All solutions were used for electrospinning in less than 72 h after their preparation. In this paper, from now on, the term PL x:y, which demonstrates the hybrid solution composition, refers to a solution containing x% PAN and y% lignin. Pure PAN solution (10 wt %), as a control sample, was also prepared and electrospun to be compared with the lignin-based fibers. As per our observation, electrospinning of above 10 wt % PAN solution was problematic due to needle blockage through electrospinning.

Electrospun nanofibers were produced by using an electrospinning setup consisted of a feeding pump (KDS Legato 101, KD Scientific, USA), a high voltage power supply (Gamma high voltage Inc., ranging from 0 to 50 kV), and an aluminum flat collector connected to the negative pole (ground). Electrospinning solutions were loaded into a 5 mL plastic syringe with a 21 gauge needle which was connected to the positive pole of high voltage. Constant working distance of 15 cm was applied between needle tip and collector, and feeding rates of 0.6 to 4 mL/h were used under voltage ranging from 10 to 15 kV.

Characterizations. Viscosity of solutions was measured using a rheometer (The Discovery HR-3, TA Instruments) as a function of shear rate with the range of 0.1 to 100 s^{-1} (40 mm diameter geometry with a 2° cone angle in a 51 μm truncation). A pendant drop experiment was employed for measuring surface tension of solutions in a contact angle meter (KSV CAM101), and conductivity of solutions was measured using a conductivity meter (S30 Mettler Toledo SevenEasy). It must be pointed out that all the measurements on solutions were carried out at room temperature.

The morphology of electrospun fibers was studied using field emission scanning electron microscopy (FE-SEM, Zeiss Supra 55VP with Gemini Column). Average fiber diameter was calculated by measuring the diameter of at least 100 random selected fibers in the SEM images using ImageJ software and IBM SPSS Statistics. In the case of beaded fibers, bead-free parts of the fibers in the SEM images were considered for the aforementioned measurements and calculations. Similarly, the average size of beads was also measured and calculated by measuring the major diameter of 50 elliptical beads in each SEM image. Differential scanning calorimetry (DSC, TA
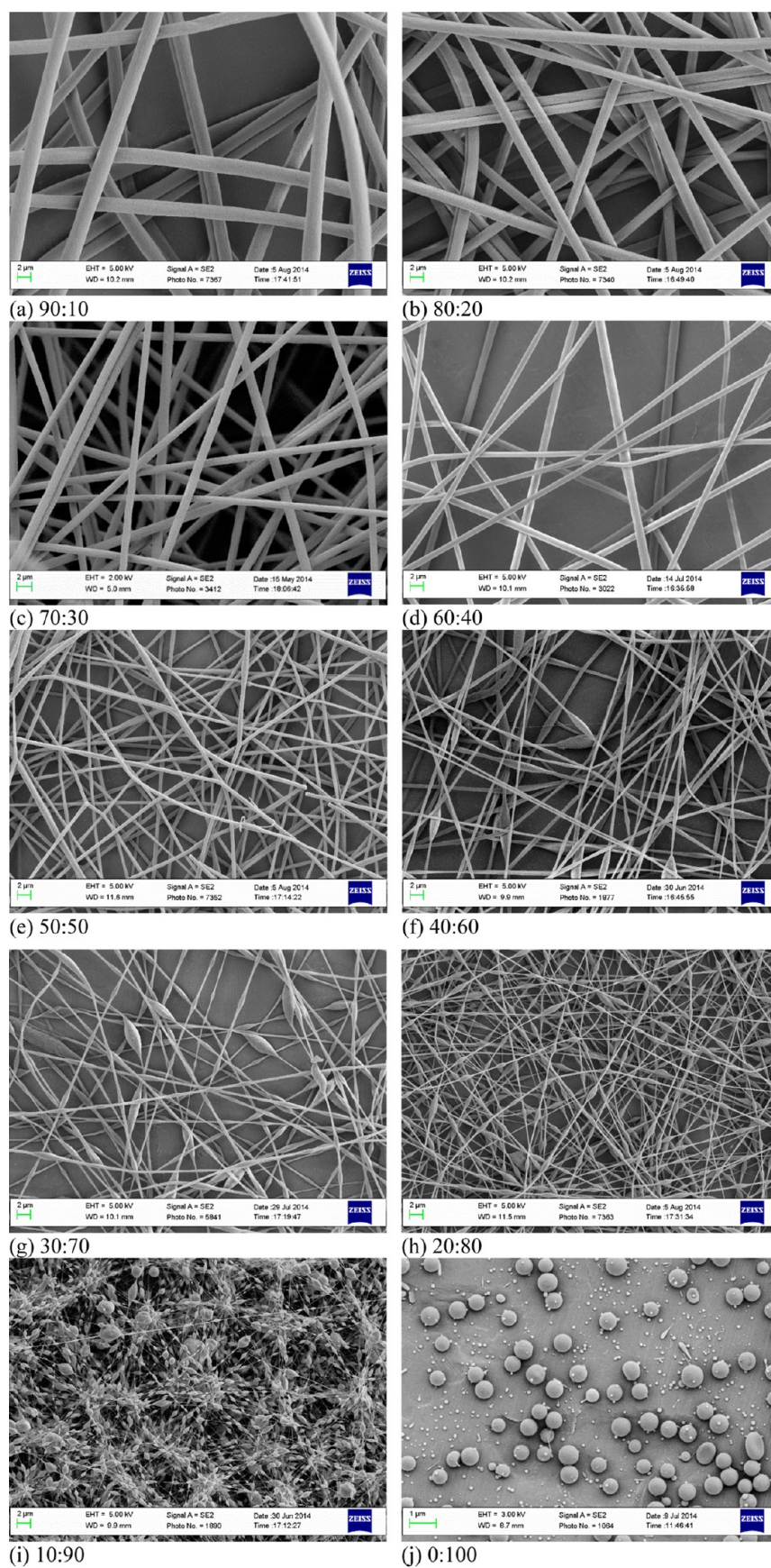
Figure 1. SEM images of electrospun lignin based fibers from 18 wt % solutions with PAN to lignin ratios of (a) 90:10, (b) 80:20, (c) 70:30, (d) 60:40, (e) 50:50, (f) 40:60, (g) 30:70, (h) 20:80, (i) 10:90, and (j) 0:100.

Table 2. Various PAN/Lignin Solution Properties and the Corresponding Properties of Resultant Electrospun Fibers

solutions					electrospun fibers	
total solution concentration (wt %)	PAN/lignin ratio	viscosity (Pa·s) (in a constant shear rate of 10 s^{-1})	surface tension (mN/m)	conductivity (μS/cm)	morphology	average fiber diameter (nm)
18	90:10	6.958	40.54 ± 0.04	109.6	uniform fibers	2240
18	80:20	4.050	40.16 ± 0.87	102.7	uniform fibers	1666
18	70:30	1.577	38.31 ± 0.17	94.3	uniform fibers	1100
18	60:40	0.498	35.28 ± 0.18	87.0	uniform fibers	738
18	50:50	0.278	35.61 ± 0.31	77.6	uniform fibers	603
18	40:60	0.127	35.24 ± 0.61	74.7	beaded fibers	390
18	30:70	0.074	34.29 ± 0.02	68.4	beaded fibers	367
18	20:80	0.028	29.22 ± 0.03	67.2	beaded fibers	201
18	10:90	0.009	31.22 ± 0.28	66.1	beaded fibers	61
18	0:100	0.002	29.13 ± 0.04	31.1	sprayed particles	
25	50:50	3.165	35.89 ± 0.68	76.0	uniform fibers	2254
25	40:60	0.988	35.19 ± 0.12	63.4	uniform fibers	2277
25	35:65	0.427	34.89 ± 0.26	51.8	uniform fibers	1396
25	30:70	0.224	33.51 ± 0.31	44.7	beaded fibers	942
25	20:80	0.063	33.35 ± 0.11	39.4	beaded fibers	362
25	10:90	0.018	33.84 ± 0.29	31.5	beaded fibers	61

Instruments Q200) was used to examine the thermal properties of electrospun nanofibers in which ∼5 mg of electrospun fibers was placed in the DSC aluminum pan, and heated from room temperature up to 380 °C with the heating rate of 10 °C/min. Additional thermal analysis was performed with thermal gravimetric analysis (TGA, TA Instruments Q50); the same amount of specimen was used, and heated from room temperature up to 600 °C under nitrogen atmosphere. Attenuated total reflectance Fourier transform infrared spectroscopy (ATR-FTIR, Vertex 70, Bruker) was used in a wavelength range of 4000 to 600 cm^{-1} to study the chemical characteristics of resultant electrospun fibers.

■ RESULTS AND DISCUSSIONS

Electrospinability and Rheological Properties of Lignin-based Solutions. We found that electrospinning of pristine lignin solution in DMF is challenging and results in electrospraying of the solution and forming spherical droplets with no fiber collectable (Figure 1j). It was observed that the fiber formation starts by introducing PAN into the spinning solutions. Various concentrations of PAN/lignin were prepared and examined for their electrospinability. The concentration 35 wt % was found as an upper limit for PAN/lignin solution concentration, since further increasing the solution concentration resulted in highly viscose solutions containing some undissolved solid polymers.

A wide range of parameters affect the electrospinning process. Apart from processing parameters such as voltage and spinning distance, material parameters such as inherent properties of polymer in hybrid solutions can play a critical role in determining the electrospinability of the polymer itself, and controlling the morphology of fabricated fibers. To explore the effect of material parameters on the electrospinability of lignin-based solutions, rheological behavior of the solutions was studied by measuring their viscosity (η), surface tension (γ), and conductivity (σ). These parameters for each individual electrospinning solution are summarized in Table 2.

As regards 18 wt % solutions, it can be seen that increasing the lignin content of solutions from 10 to 100% significantly decreases the conductivity of solutions from 109.6 to 31.1 μS/cm. It is worth mentioning that the conductivity of DMF used in this work (0.74 μS/cm) significantly increased by dissolution of PAN in, whereas the addition of lignin to the PAN solution

in DMF had a reverse influence on the overall conductivity and dramatically decreased it. Formation of beaded electrospun lignin fibers is more likely when the electrical conductivity of solution is lower and this is in consistent with what has recently been reported in the literature.[24] This is in line with a gradual decline in surface tension of solutions from 40.54 to 29.13 mN/m, respectively. According to our observations, it was found that the formation of beaded PAN/lignin fibers occurs at lower conductivities and lower surface tensions. This could be due to the effect of capillary breakup in solutions with lower surface tension that lead to bead and, finally, droplet formation.[38] Solutions containing a lignin portion higher than 50% resulted in conductivities and surface tensions of lower than 77.6 μS/cm and 35.61 mN/m, respectively. These can be considered as the critical points for shift from uniform fibers to beaded fibers in a total polymer concentration of 18 wt % in solution. In other words, these thresholds can be assumed as the starting points of possible capillary breakup instabilities. Likewise, similar trend can be seen for 25 wt % solutions, where increasing lignin component of the polymer solution has led to a remarkable decrease in solution conductivity and a gradual reduce in surface tension. Nevertheless, with regard to 25 wt % solutions, the formation of beaded fibers has started from solution with 70% lignin content, whereas in the case of 18 wt % solutions, beaded fibers were formed at lower lignin contents, i.e., 60%. This confirms that apart from conductivity and surface tension that have critical roles in electrospinning behavior of solutions, solution concentration and in effect viscosity are both also very important material variables governing the formation of either beaded or uniform fibers.

In terms of 18 wt % solutions, it is observed that further addition of lignin to the hybrid solution reduces the dynamic viscosity of solution. Solutions with higher lignin content enjoy lower viscosities. It has been demonstrated that the higher viscosity a solution has, the more likely is the formation of bead-free fibers.[39] We observed that the addition of low molecular weight organosolv lignin compared to PAN with higher molecular weight, caused a significant drop in the viscosity of solution from η = 21.65 Pa·s for 18 wt % pure PAN solution to η = 6.958 Pa·s for the PAN/lignin 90:10 solution. In
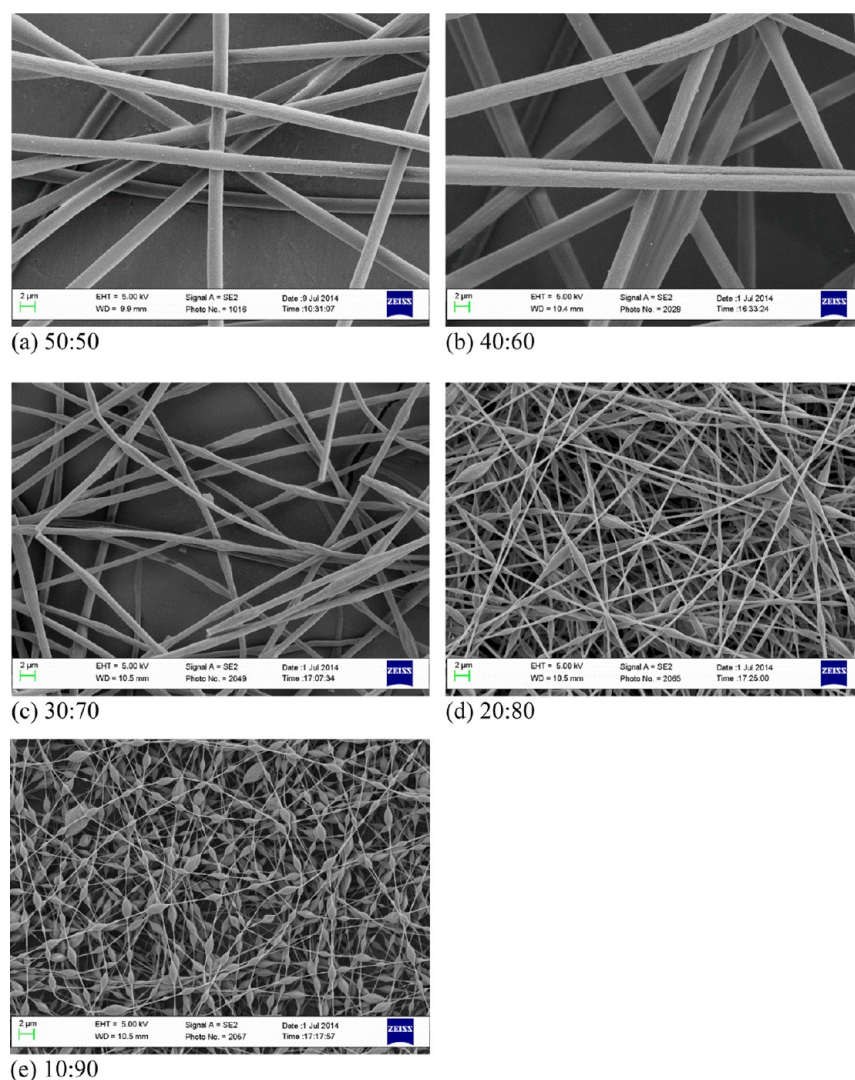
Figure 2. SEM images of electrospun lignin based fibers from 25 wt % solutions with PAN to lignin ratios of (a) 50:50, (b) 40:60, (c) 30:70, (d) 20:80, and (e) 10:90.

fact, the viscosity-reducing nature of lignin derivatives has been attributed to their aromatic hyper-branched structure.[40]

When the PAN content went beyond 50% in 25 wt % solutions, both the solution preparation and the electrospinning were found to be difficult, as a result of higher viscosity of the solutions. Therefore, we have only examined the electro-spinability of 25 wt % solutions with lignin content of equal and more than 50%. It is worth to mention that in electrospinning of solutions with higher viscosity, higher voltage had to be applied to overcome the high surface tension of the polymer solution.

Morphology of PAN/Lignin Blend Electrospun Fibers.
Unlike white PAN electrospun fibers, brown nanofibers were obtained through electrospinning of PAN/lignin hybrid solutions. Figures 1 and 2 show SEM images of as-spun lignin fibers and electrosprayed particles resulted from 18 and 25 wt % PAN/lignin hybrid solutions, respectively. As can be clearly seen from Figure 1, uniform fibers are formed from solution blends containing up to 50% lignin, whereas a higher amount of lignin in the solution resulted in beads-on-string structures. As Figure 1 shows, with the rise in the lignin proportion in the composition, the number of beads on a certain length of fiber grow gradually, and concurrently the distance between beads

shorten. At the same time, the morphology of beads changed from an almond shaped to a more spherical shape. Eventually, a complete sphere in electrosprayed pure lignin solution in form of droplets was seen. Nonetheless, as can be seen in Figure 3, bead sizes decrease with increasing the lignin content of hybrid electrospun fibers. This can be attributed to the role of
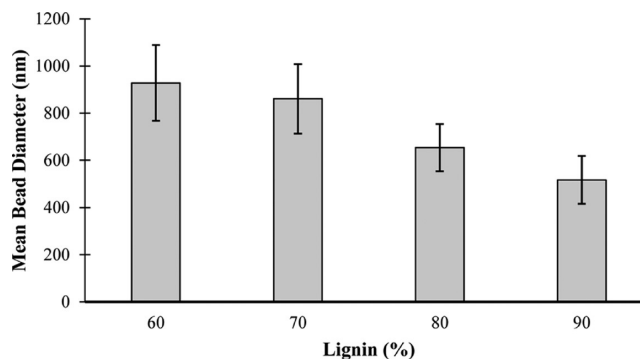

Figure 3. Average bead diameters of electrospun fibers versus lignin percentage in solutions with total concentrations of 18 wt %.

viscosity, which decreases with increasing the lignin content in the solution (Table 2), and thereby results in formation of smaller beads on the fiber.[39] Likewise, a similar trend is observed for electrospun fibers from 25 wt % solutions (Figure 2).

As beaded fibers only appeared in solutions containing more than 50% lignin in 18 wt % solutions, only electrospinning of solutions with lignin content higher than 50% was conducted in the case of 25 wt % solutions, to see whether higher solution concentration (25 wt %) help to eliminate beads in those high lignin content solutions. Interestingly, raising the overall concentration of solution from 18 to 25 wt % resulted in elimination of beads in solution containing 60% lignin, whereas bead formation was observed again when the lignin content reached to 70%. Considering viscosity of solutions (Table 2), it can be seen that the viscosity of 18 wt % solution with 60% lignin (0.127 Pa·s) is approximately one-eighth that of the 25 wt % solution (0.988 Pa·s). In other words, increasing total concentration of hybrid solution boosted the formation of uniform, bead-free fibers with higher amounts of lignin. Nonetheless, the presence of 70% lignin in the composition of polymer solution resulted in some minor beads on the surface of the fibers.

Figure 4 illustrates the correlation between the diameter of electrospun fibers and the lignin content of 18 and 25 wt %
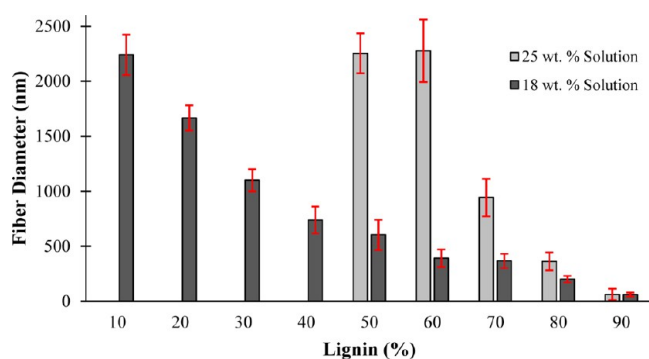

Figure 4. Average diameters of electrospun fibers versus lignin percentage in hybrid solutions with total concentrations of 18 and 25 wt %.

solutions. It can be clearly seen that the fibers diameter contract substantially with increase in lignin content. The more lignin in the composition of solutions, the thinner fibers have formed.

The diameter measurements from SEM images showed that electrospun fibers from 18 and 25 wt % solutions have diameters ranging from nanometer to micrometer scales; 61 to 2240 nm and 61 to 2254 nm, respectively. It is interesting to note that fibers produced from 18 wt % lignin-based solution with only 10% lignin content had approximately similar diameter to those electrospun from 25 wt % solution containing 50% lignin content, 2240 and 2254 nm, in the order already mentioned. As already demonstrated in the literature,[41] increasing the solution concentration would result in larger fiber diameter.

Viscosity and stress measurements as a function of shear rate for 18 wt % PAN/lignin solutions (Figure 5a,b) reveals that loading more lignin in bicomponent solutions causes an obvious shear thinning which intensely happens in solutions with lignin concentrations less than 30%. In addition, non-Newtonian fluid behavior can be recognized for those solutions with higher viscosity, lignin content of less than 30%. This can be attributed to the fact that some of entangled polymer chains in the solution become oriented under flow to the shear direction.[42,43] In contrast, for low viscosity solutions (with lignin more than 20%), shear thinning effect decreases after the shear rate of 10 s^{-1}, indicating that the viscosity of these solutions remain steady and is independent of shear force. Therefore, lignin-based solutions with lignin contents more than 20% can be classified as the fluids following Newtonian fluid behavior.

Phase Behavior of PAN/Lignin Blend Electrospun Fibers. Glass transition temperature (T_g) and decomposition temperature (T_m) were employed to study the phase behavior of polyblend electrospun fibers. Figure 6 illustrates differential scanning calorimetric (DSC) curves of 10 wt % PAN and various electrospun fibers obtained from 18 wt % solution blends with different lignin contents. The T_g range of the composite electrospun fibers is shown in the inset graph. As can be seen from the inset graphs, all the lignin-based electrospun fibers with various PAN/lignin ratios have shown only one single T_g rather than two T_g values for each individual polymer (please also see Figure S1 of the Supporting Information). This reveals that PAN and lignin are miscible with no phase separation during the fiber formation. As can be also found from Figure 6, presence of lignin in the polyblend electrospun fibers has raised the T_g, and endothermic peak has moved toward higher temperatures. According to the graph, composite fiber samples that contain lignin enjoy higher T_g's in a broader temperature range than the pure PAN fibers. The higher and wider T_g range observed for samples with lignin mainly arises from the highly aromatic and complex structure of lignin as well as large number of hydrogen bonds in the main chain.[40,44] Besides, it has been proposed that[45] an increase in T_g after polymer blending shows the compatibility and phase miscibility of the two polymers in blends. A shift in T_g with increasing lignin content is also attributed to the molecular level interactions of PAN and lignin that occur during the thermal treatments.

The decomposition temperature (T_m) and heat of fusion (ΔH_m) for blends are demonstrated in Table 3. As is clear, the lowest temperature at which an exothermic peak has appeared is approximately 294 °C, which refers to electrospun pure PAN fibers. Addition of only 10% lignin to the PAN solution led to a sudden increase in T_m to 301 °C for the resultant electrospun fibers. A higher lignin ratio in the composite fibers resulted in a larger decomposition point, about 314 °C for PAN/lignin 10:90. This is a 20 °C increase in decomposition temperature from 100% PAN fibers to PAN/lignin ratio of 10:90. At the same time, a remarkable decrease in heat of fusion (from 503 to 60 J/g) is identified with rising the lignin portion in the composite fibers from 10% to 90%. Besides, when the lignin content of the electrospun lignin-based fibers increases, the exothermic peaks change from sharp to broad peaks. The same pattern is observed in case of exothermic peaks of electrospun PAN/lignin fibers obtained from 25 wt % solutions shown in Figure S2 of the Supporting Information.

A clear increase in decomposition temperatures and a corresponding decrease in heat of reactions can be realized with rise in lignin ratio of composite fibers. Although lignin is known as an amorphous polymer,[46] the increase in the T_m of PAN/lignin fibers with increasing the lignin content as well as the decrease in the ΔH_m could be due to the intermolecular interactions between PAN and lignin chains particularly when
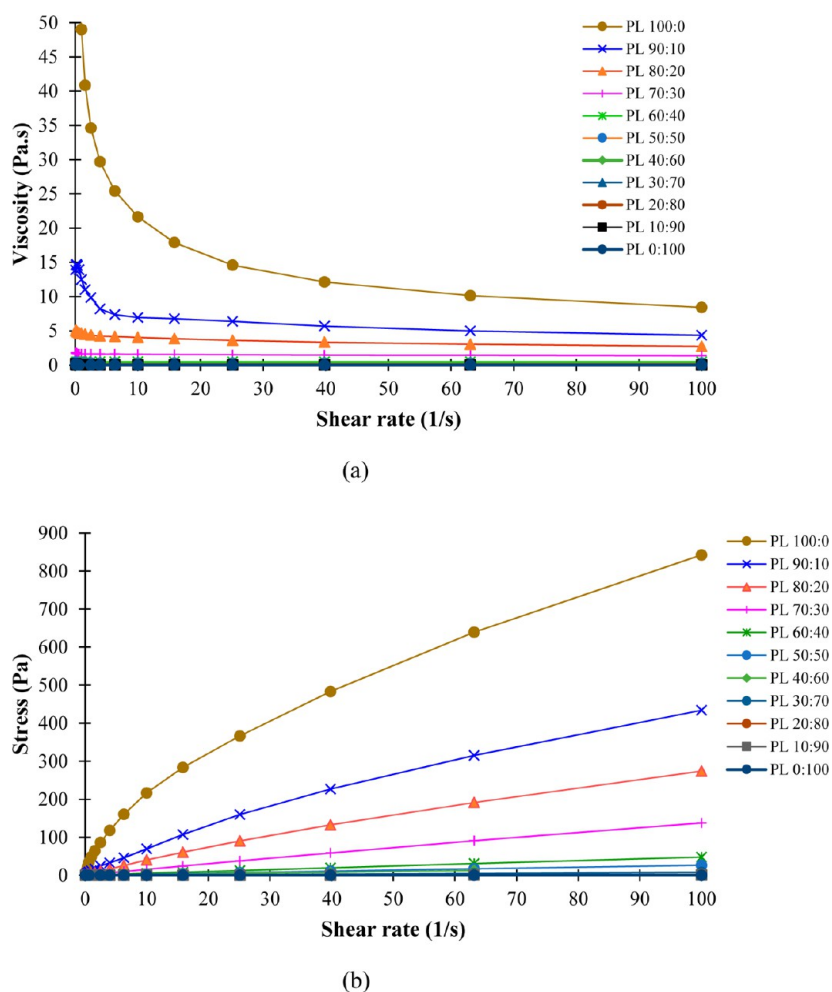
(a)

(b)

Figure 5. (a) Viscosity and (b) stress as a function of shear rate for different PAN/Lignin ratios in 18 wt % solutions.
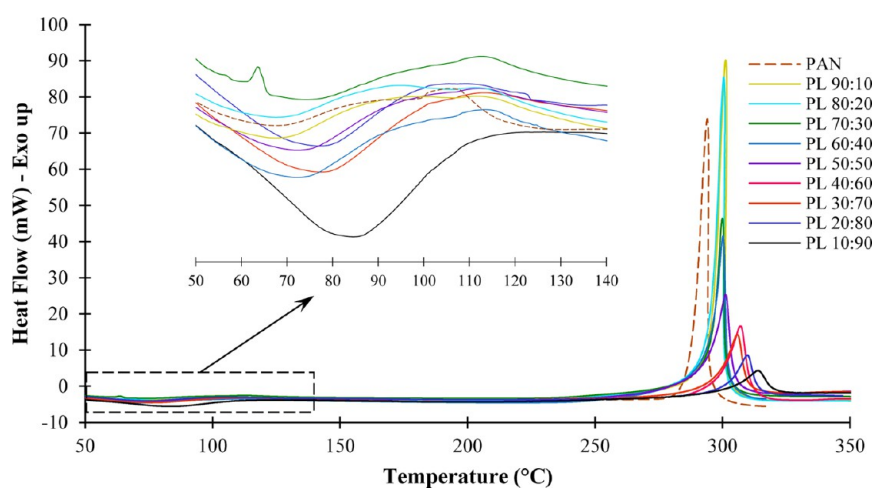

Figure 6. DSC curves of PAN/lignin electrospun fibers with different lignin contents from 18 wt % solutions and a reference curve for electrospun pure PAN fibers from 10 wt % solution. (The inset graph shows glass transition temperature range (T_g) of composite electrospun fibers.)

Table 3. Degradation Temperature (T_m) and Enthalpy of Fusion (ΔH_m) for Various PAN/Lignin (PL) and Pure PAN Electrospun Fibers from 18 and 10 wt % Solutions, Respectively

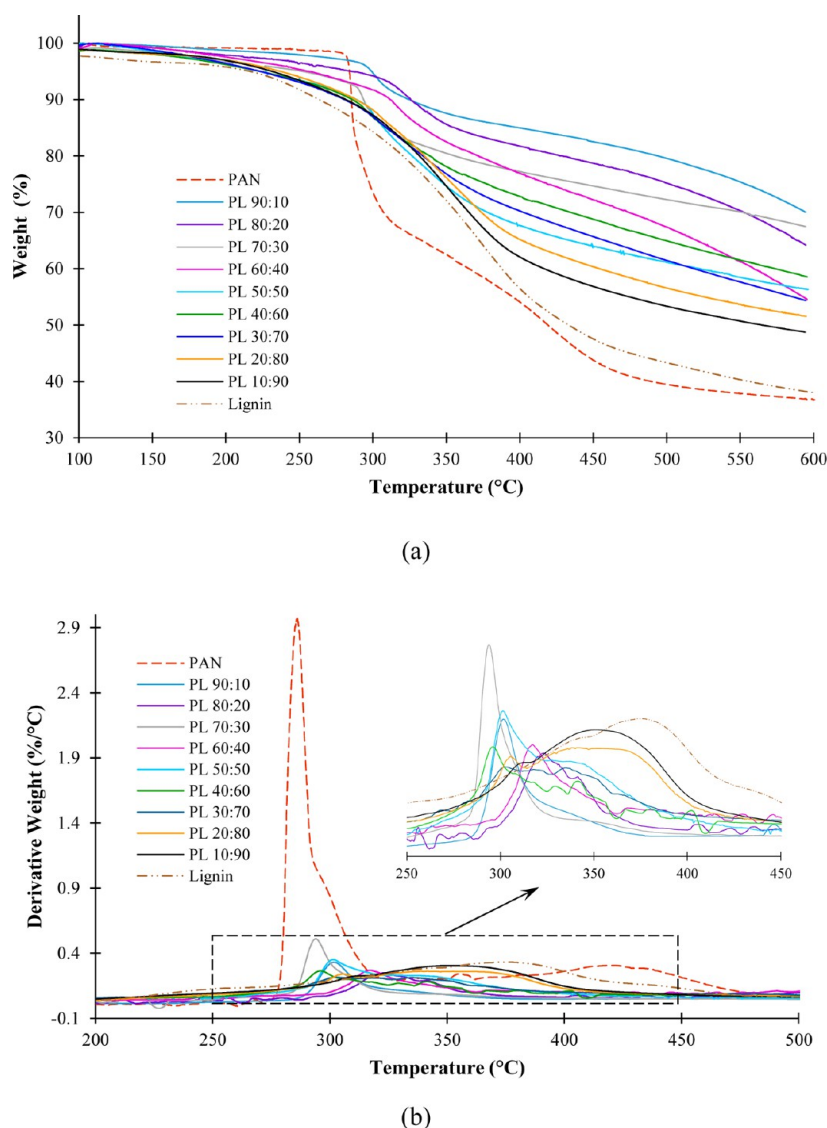|	PAN	PL90:10	PL80:20	PL70:30	PL60:40	PL50:50	PL40:60	PL30:70	PL20:80	PL10:90
T_m (°C)	294	301	301	300	300	301	307	306	310	314
ΔH_m (J/g)	241	503	500	402	351	306	259	186	115	60

(a)

(b)

Figure 7. TGA curves of (a) PAN/lignin electrospun fibrous with different lignin content obtained from 18 wt % solutions and corresponding curve for pure lignin powder and electrospun pure PAN fibers from 10 wt % solution, (b) derivative weights of the same samples. (The inset graph show a focused view of composite electrospun fibers.)

Table 4. Maximum Weight Loss Rate (R), Carbon Yield at 600°C (C), Temperature of Major Mass Loss (T_{max}), activation energy (E_a), and the corresponding R^2 values in kinetic plots of various PAN/Lignin (PL) and Pure PAN Electrospun Fibers from 18 and 10 wt % Solutions, Respectively

	PAN	PL90:10	PL80:20	PL70:30	PL60:40	PL50:50	PL40:60	PL30:70	PL20:80	PL10:90
R (%/°C)	2.97	0.33	0.25	0.51	0.27	0.35	0.26	0.22	0.26	0.30
C (%)	37	70	64	67	55	56	59	54	52	49
T_{max} (°C)	286	302	323	294	317	301	296	303	306	313
E_a (kJ/mol) (R^2)	117 (0.99)	49 (0.97)	42 (0.96)	35 (0.81)	32 (0.95)	28 (0.97)	23 (0.94)	25 (0.98)	32 (0.98)	23 (0.99)

being heat treated during thermal analysis, in which thermochemical reactions between polyaromatic lignin and linear PAN play a significant role. Meanwhile, it should be pointed out that the α-ether linkages available in the ether chains of the lignin structure will be cleaved at higher temperatures of above 300 °C. This further confirms the fact that the presence of lignin can increase the T_m in lignin-based electrospun fibers.[33]

Pyrolysis Behavior of PAN/Lignin Blend Electrospun Fibers. Thermal stability of the PAN/lignin composite fibers was studied using thermogravimetric analysis (TGA). Figure 7a

shows the TGA profiles of electrospun PAN and PAN/lignin fibers. The corresponding derivatives can be seen in Figure 7b. As can be seen from the graphs, pure PAN nanofibers were fairly stable up to 286 °C without any significant weight loss. The first major degradation of pure PAN fibers occurred at around 286 °C and the second one at about 420 °C. Comparing PAN/lignin composite fibers with pure PAN fibers, one can see that composite fibers show a continuous weight loss with increasing the temperature. Nevertheless, the first major degradation temperature has shifted toward higher temperatures. This is in consistent with the aforementioned
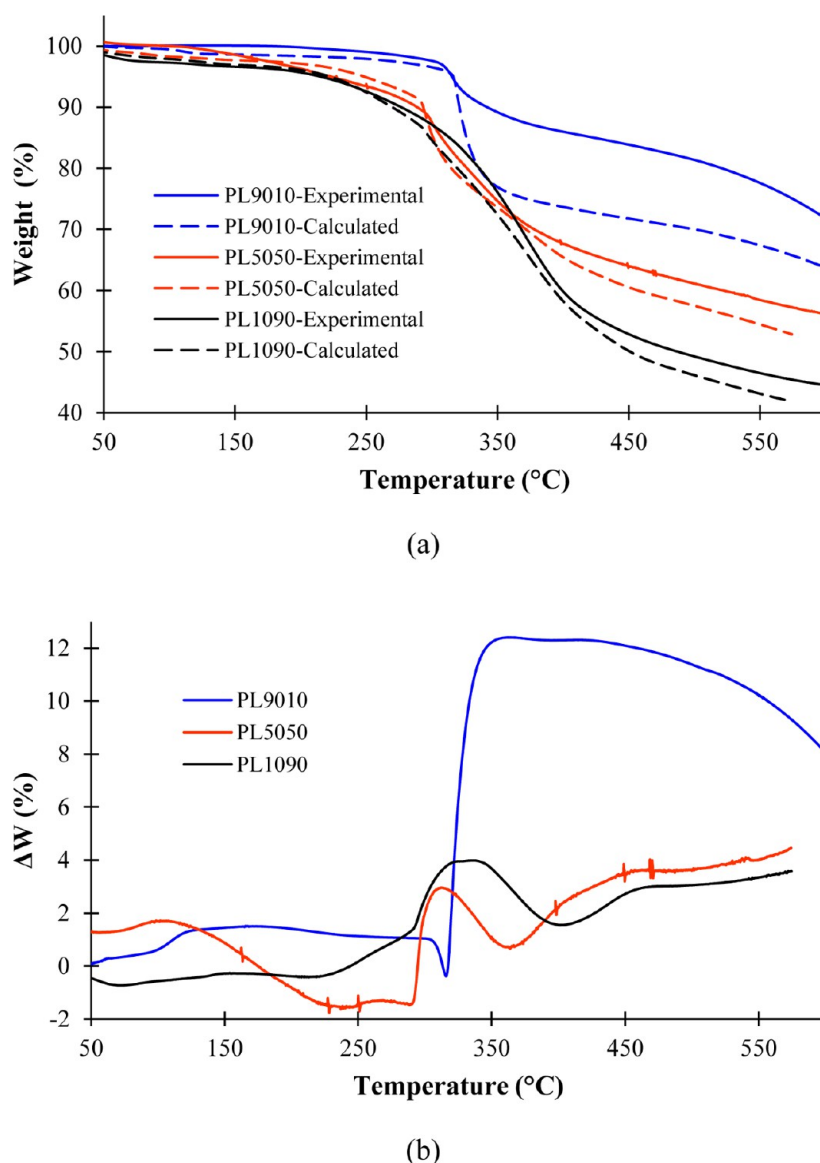
(a)

(b)

Figure 8. (a) Comparison between experimental and calculated weight loss values, and (b) ΔW values obtained from thermogravimetric curves of PAN/lignin electrospun fibrous with different lignin content obtained from 18 wt % solutions.

DSC results in which T_m raised upon increase in the lignin content of composite fibers. For instance, the first main weight loss of electrospun PAN/lignin 90:10 was recorded at 302 °C, and that of PAN/lignin 10:90 at 313 °C, both higher than that of pure PAN by 15 and 27 °C, respectively. With respect to the second important weight loss of lignin-based fibers, it appears in a lower temperature compared to that of pure PAN. As can be found from the curves, the second major degradation of electrospun PAN/lignin 10:90 was observed at 351 °C, which is 69 °C lower than that of pure PAN.

Regarding the weight loss derivatives shown in Figure 7b, one can easily see an extremely sharp derivative peak for electrospun pure PAN fibers (around 286 °C) showing a sudden major weight loss, followed by a small broad peak (about 420 °C). However, addition of more lignin into the hybrid polymer system, resulted in the broader peaks.

Table 4 summarizes the parameters derived from TGA curves, namely the maximum weight loss rate (R), temperature of major weight loss (T_{max}), carbon yield (C), and activation energy of pyrolysis (E_a). The Coats and Redfern approach[47]

was employed to calculate E_a of pyrolysis for pure PAN and polyblend electrospun lignin-based fibers. According to eq 1, where α is the mass conversion, E_a is activation energy of pyrolysis, R is the universal gas constant (8.314 J/(mol·K)), T is the temperature, and C is a constant, $\ln(-\ln(1 - \alpha)/T^2)$ versus $1/T$ gives a straight line in which E_a can be obtained from the slope of the line.

$$\ln\left(\frac{-\ln(1 - \alpha)}{T^2}\right) = C - \frac{E_a}{RT} \tag{1}$$

The results (Table 4) show that the E_a of pyrolysis for the polyblend PAN/lignin fibers with different lignin contents is significantly lower than that of pure PAN fiber. Clearly, this indicates that more energy was consumed for the degradation of PAN fibers, whereas a remarkably lower amount of energy has driven the degradation reactions in the lignin-based fibers. This can suggest the different nature of the reactions taking place in the polyblend PAN/lignin fibers during the thermal decomposition. As regards the linear structure of PAN, the
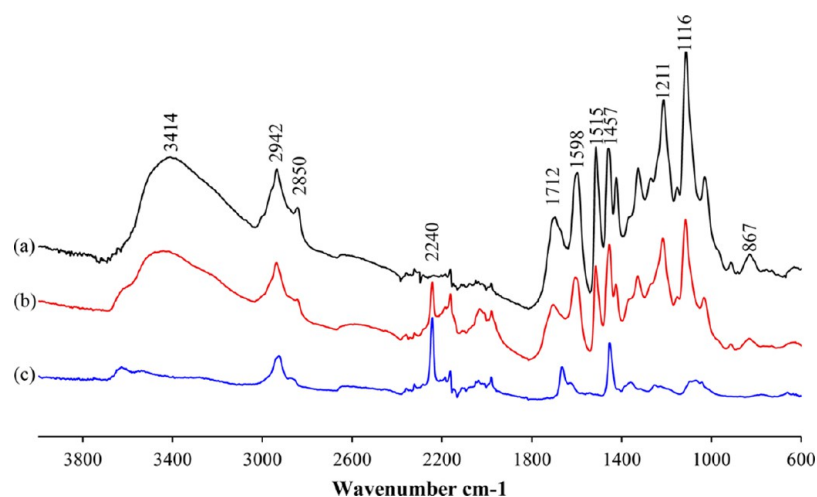
Figure 9. FTIR spectra of (a) pure lignin powder, (b) electrospun 18 wt % PAN/lignin 40:60, and (c) 10 wt % pure PAN fibers.

typical thermal reaction is cyclization, whereas in the case of lignin with a hyper-branched aromatic heterogeneous structure, it is hypothesized that there are several parallel reactions contributing in the thermal decomposition of lignin-based fibers.[48] This can be further confirmed by the fact that E_a essentially depends on the nature of polymer as well as its chemical structure and degree of crystallinity.[49] The lower E_a of polyblend PAN/lignin fibers compared to that of pure PAN fibers may also be attributed to the amorphous structure of lignin that requires lower energy through thermal decomposition. In addition, the energy required for cleavage of triple bonds in the nitrile group of PAN probably plays a major role in the higher E_a of PAN; E_a decreases with reducing the amount of PAN in the fiber composition. Therefore, E_a depends on the composition of the polyblend and changes with altering the ratios of PAN and lignin in fibers. The result suggests that the differences in thermal stability of pure PAN and PAN/lignin fibers could be due to the different nature of thermal degradation reactions, evidenced by various E_as.

The maximum weight loss rate (R) of electrospun pure PAN fibers is about 3 wt %/°C, whereas PAN/lignin fibers showed lower maximum weight loss rates ranging from 0.2 to 0.5 wt %/°C, a significant decrease of 15 to 6 times. This reveals that the decomposition of composite PAN/lignin fibers is more difficult than that of pure PAN fibers. In fact, lignin-based fibers experience slower thermal decomposition over a broad range of temperatures compared to pure PAN fibers with rapid thermal decomposition in a shorter range of temperatures. As already discussed above regarding the decomposition temperatures of composite fibers, structural properties of lignin may possibly be responsible for the difficulty in decomposition of fibers containing lignin.[50] As regards the carbon yield, we found that the slower rate of degradation of lignin-based fibers accompanied by higher carbon yield at final temperature of 600 °C. Considering the TGA graph for each individual polymer, the decomposition behavior of composite PAN/lignin fibers can be explained by the synergistic effect of the combined polymers on the decomposition reactions through pyrolysis. When a combination of two or more chemical substances results in a total effect greater than the sum of their individual effects, there might be a cooperative interaction that is known as the synergistic effect. The synergistic effect taking place during the copyrolysis of PAN and lignin can be estimated by the subtraction of calculated weight loss (W_{cal}) from

experimental weigh loss (W_{exp}) values by using eq 2.[51,52] W_{exp} has already been obtained from TGA, but W_{cal} can be calculated from the sum of each individual polymer weight loss (W_{lignin} and W_{PAN}) multiplied by their mass fractions in the blend (M_{lignin} and M_{PAN}), as shown in eq 3.

$$\Delta W = W_{exp} - W_{cal} \qquad (2)$$

$$W_{cal} = M_{lignin} W_{lignin} + M_{PAN} W_{PAN} \qquad (3)$$

To investigate the synergistic effect of polyblend PAN/lignin fibers, three ratios of 90:10, 50:50, and 10:90 were selected. As shown in Figure 8a, the experimental weight loss values are mostly greater than that of calculated. As already noted, this may indicate the possible synergistic effect taking place between lignin and PAN. In the range of temperatures recorded by TGA, the experimental values of weight losses are mostly higher than the calculated ones, which are more significant at higher temperatures. Therefore, the differences of W_{exp} and W_{cal} are positive values (Figure 8b) showing a positive synergistic effect between two individual polymers in the lignin-based electrospun fibers, which results in deceleration of thermal decomposition and also a larger solid residue remaining after the pyrolysis. This might suggest that combining PAN and lignin can hinder the decomposition of each individual polymer. As lignin has a three-dimensional heterogeneous aromatic molecular structure, it can be postulated that it may provide some traps and gaps among the polymer chains in the blend, by which less volatile compounds are able to abandon the polyblend structure.[51] Therefore, a lower quantity of volatiles can be released in a certain period of time, resulting in a larger char amount and higher W_{exp}.

Functional Groups in Electrospun Composite PAN/Lignin Fibers (ATR-FTIR). FTIR spectra of electrospun fibers obtained from a PAN/lignin ratio of 40:60 in 18 wt % solution are shown in Figure 9 along with the reference spectra for organosolv lignin powder and electrospun pure PAN fibers. Considering the pure lignin spectrum (a), a relatively week band at 867 cm^{-1} originates from C—H deformations. Also, C—O stretching bonds can be assigned to the peak at around 1211 cm^{-1}. The two bands around 1515 and 1600 cm^{-1} are corresponding to vibrations of aromatic rings in phenylpropane units, i.e., aromatic ring deformations and aromatic stretching bands, respectively. The peaks observed at around 1712 and 1365 cm^{-1} are associated with unconjugated carbonyl groups

and phenolic hydroxyl groups, respectively,[53] which are originally formed during the ethanol organosolv isolation process of the hardwood lignin.[54] A broad peak around 3400 cm^{-1} indicates the stretching vibrations of strong bonds in hydroxyl groups (O—H), which is of constituting groups of phenolic and aliphatic structures.[53] In PAN/lignin fibers (spectrum b), it can be seen that this peak has shifted toward higher wavenumbers, i.e., 3440 cm^{-1}, with less sharpness, due to the decrease in lignin content compared to pure lignin spectrum, and increasing the stretching vibration of O—H after blending with PAN. Apart from the fingerprint regions of each individual polymer, some similar functional groups, which are available in both polymers, have peaked at the same regions in the spectra. For instance, the two peaks around 2942 and 2850 cm^{-1} in all three spectra, generally arise from C—H stretching vibrations in both polymers.[54] With respect to spectrum c, the typical sharp peak at 2240 cm^{-1} can be related to C≡N groups in the structure of the pure PAN fiber;[55] nonetheless, it is weakened for PAN/lignin nanofibers due to the presence of lignin as the predominant portion in the blend. The spectrum of a polyblend comprising both lignin and PAN shows characteristics of both polymers; however, because there is no indication of any new peak in the FTIR spectrum of lignin-based electrospun fibers, it seems that no new functional group has formed in the PAN/lignin polyblend, and there is only physical interaction between two polymers.

CONCLUSION

In the present work, we used hardwood organosolv lignin that not only is a high purity biorenewable polymer but also is produced through a more environmentally friendly pulping process. Electrospinning solutions with various compositions of organosolv lignin and PAN were prepared. Solution rheology was examined by measuring the critical parameters of viscosity, surface tension, and electrical conductivity of solutions. The PAN/lignin solution blends properties as well as scanning electron microscopy images of the resultant composite fibers, was used to determine the critical points for transition from nonhomogenous beaded fibers to bead-free uniform fibers. It was found that lignin-based composite fibers enjoy higher decomposition temperatures followed by a larger carbon yield compared to pure PAN fibers. A gradual weight loss was seen in the pyrolysis of PAN/lignin fibers over a broader range of temperature compared to pure PAN fibers with a sudden sharper weight loss. Thermal decomposition of lignin and PAN showed a significant synergistic effect between two constituting polymers in the lignin-based electrospun fibers. A lower activation energy was found for the pyrolysis of lignin-based fibers compared to pure PAN fibers. The findings of this study showed that although organosolv lignin, as a low-cost precursor of carbon fiber, enjoys low molecular weight compared to PAN, it is feasible to employ it in the polyblends for the purpose of carbon fiber production, which is the subject of our current research, and will be reported in the future.

ASSOCIATED CONTENT

Ⓢ Supporting Information

DSC curves of pure organosolv lignin powder and PAN/lignin electrospun fibers from 25 wt % solutions. This material is available free of charge via the Internet at http://pubs.acs.org/.

AUTHOR INFORMATION

Corresponding Author

*M. Naebe. E-mail: minoo.naebe@deakin.edu.au. Tel: +61 3 52271410.

Notes

The authors declare no competing financial interest.

ACKNOWLEDGMENTS

REFERENCES

(1) Thunga, M.; Chen, K.; Grewell, D.; Kessler, M. R. Bio-renewable precursor fibers from lignin/polylactide blends for conversion to carbon fibers. *Carbon* **2014**, *68*, 159−166.

(2) Luckachan, G. E.; Pillai, C. K. S. Biodegradable polymers — A review on recent trends and emerging perspectives. *J. Polym. Environ.* **2011**, *19* (3), 637−676.

(3) Kubo, S.; Kadla, J. F. Lignin-based carbon fibers: Effect of synthetic polymer blending on fiber properties. *J. Polym. Environ.* **2005**, *13* (2), 97−105.

(4) Avérous, L.; Pollet, E. Biodegradable polymers. In *Environmental Silicate Nano-Biocomposites*; Avérous, L., Pollet, E., Eds.; Springer: London, 2012; pp 13−39.

(5) Feldman, D. Lignin and its polyblends — A review. In *Chemical Modification, Properties, and Usage of Lignin*; Hu, T. Q., Ed; Plenum: New York, 2002; pp 81−99.

(6) Valizadeh, M.; Hosseini Ravandi, S. A.; Ramakrishna, S. Recent advances in electrospinning of some selected biopolymers. *J. Text. Polym.* **2013**, *1* (2), 70−84.

(7) Hatakeyama, H.; Hatakeyama, T. Lignin structure, properties, and applications. In *Biopolymers: Lignin, Proteins, Bioactive Nano-composites*; Abe, A., Kobayashi, S., Dusek, K., Eds.; Springer: Heidelberg, 2010; pp 1−63.

(8) Crist, D. R.; Crist, R. H.; Martin, J. R. A new process for toxic metal uptake by a kraft lignin. *J. Chem. Technol. Biotechnol.* **2003**, *78* (2−3), 199−202.

(9) Khan, M. A.; Ashraf, S. M.; Malhotra, V. P. Development and characterization of a wood adhesive using bagasse lignin. *Int. J. Adhes. Adhes.* **2004**, *24* (6), 485−493.

(10) Lora, J. H.; Glasser, W. G. Recent industrial applications of lignin: A sustainable alternative to nonrenewable materials. *J. Polym. Environ.* **2002**, *10* (1−2), 39−48.

(11) Katsumata, K.; Meshitsuka, G. Modified kraft lignin and its use for soil preservation. In *Chemical Modification, Properties, and Usage of Lignin*; Hu, T. Q., Ed.; Springer: New York, 2002; pp 151−165.

(12) Sannigrahi, P.; Ragauskas, A. J. Fundamentals of biomass pretreatment by fractionation. In *Aqueous Pretreatment of Plant Biomass for Biological and Chemical Conversion to Fuels and Chemicals*; Wyman, C. E., Ed.; John Wiley & Sons: London, 2013; pp 201−222.

(13) Baker, D. A.; Rials, T. G. Recent advances in low-cost carbon fiber manufacture from lignin. *J. Appl. Polym. Sci.* **2013**, *130* (2), 713−728.

(14) Lai, C.; Zhou, Z.; Zhang, L.; Wang, X.; Zhou, Q.; Zhao, Y.; Wang, Y.; Wu, X. F.; Zhu, Z.; Fong, H. Free-standing and mechanically flexible mats consisting of electrospun carbon nanofibers made from a natural product of alkali lignin as binder-free electrodes for high-performance supercapacitors. *J. Power Sources* **2014**, *247*, 134−141.

(15) Ragauskas, A. J.; Beckham, G. T.; Biddy, M. J.; Chandra, R.; Chen, F.; Davis, M. F.; Davison, B. H.; Dixon, R. A.; Gilna, P.; Keller, M.; Langan, P.; Naskar, A. K.; Saddler, J. N.; Tschaplinski, T. J.; Tuskan, G. A.; Wyman, C. E. Lignin valorization: Improving lignin processing in the biorefinery. *Science* **2014**, *344*, 1−10.

(16) Dallmeyer, I.; Ko, F.; Kadla, J. F. Electrospinning of technical lignins for the production of fibrous networks. *J. Wood Chem. Technol.* **2010**, *30*, 315−329.

(17) Naebe, M.; Lin, T.; Tian, W.; Dai, L.; Wang, X. Effects of MWNT nanofillers on structures and properties of PVA electrospun nanofibres. *Nanotechnol.* **2007**, *18*, 1−8.

(18) Zhang, L.; Aboagye, A.; Kelkar, A.; Lai, C.; Fong, H. A review: Carbon nanofibers from electrospun polyacrylonitrile and their applications. *J. Mater. Sci.* **2014**, *49* (2), 463−480.

(19) Frank, E.; Steudle, L. M.; Ingildeev, D.; Spörl, J. M.; Buchmeiser, M. R. Carbon fibers: Precursor systems, processing, structure, and properties. *Angew. Rev.* **2014**, *53*, 2−39.

(20) Suhas; Carrott, P. J. M.; Ribeiro Carrott, M. M. L. Lignin — From natural adsorbent to activated carbon: A review. *Bioresour. Technol.* **2007**, *98* (12), 2301−2312.

(21) Lallave, M.; Bedia, J.; Ruiz-Rosas, R.; Rodríguez-Mirasol, J.; Cordero, T.; Otero, J. C.; Marquez, M.; Barrero, A.; Loscertales, I. G. Filled and hollow carbon nanofibers by coaxial electrospinning of alcell lignin without binder polymers. *Adv. Mater.* **2007**, *19* (23), 4292−4296.

(22) Norberg, I.; Nordström, Y.; Drougge, R.; Gellerstedt, G.; Sjöholm, E. A new method for stabilizing softwood kraft lignin fibers for carbon fiber production. *J. Appl. Polym. Sci.* **2013**, *128* (6), 3824−3830.

(23) Kadla, J. F.; Kubo, S.; Venditti, R. A.; Gilbert, R. D.; Compere, A. L.; Griffith, W. Lignin-based carbon fibers for composite fiber applications. *Carbon* **2002**, *40* (15), 2913−2920.

(24) Ago, M.; Okajima, K.; Jakes, J. E.; Park, S.; Rojas, O. J. Lignin-based electrospun nanofibers reinforced with cellulose nanocrystals. *Biomacromolecules* **2012**, *13*, 918−926.

(25) Teng, N. Y.; Dallmeyer, I.; Kadla, J. F. Incorporation of multiwalled carbon nanotubes into electrospun softwood kraft lignin-based fibers. *J. Wood Chem. Technol.* **2013**, *33*, 299−316.

(26) Choi, D. I.; Lee, J. N.; Song, J.; Kang, P. H.; Park, J. K.; Lee, Y. M. Fabrication of polyacrylonitrile/lignin-based carbon nanofibers for high-power lithium ion battery anodes. *J. Solid State Electrochem.* **2013**, *17*, 2471−2475.

(27) Schreiber, M.; Vivekanandhan, S.; Mohanty, A. K.; Misra, M. A study on the electrospinning behaviour and nanofibre morphology of anionically charged lignin. *Adv. Mater. Lett.* **2012**, *3* (6), 476−480.

(28) Hu, S.; Hsieh, Y. L. Ultrafine microporous and mesoporous activated carbon fibers from alkali lignin. *J. Mater. Chem. A* **2013**, *1*, 11279−11288.

(29) Gao, G.; Dallmeyer, J. I.; Kadla, J. F. Synthesis of lignin nanofibers with ionic-responsive shells: Water-expandable lignin-based nanofibrous mats. *Biomacromolecules* **2012**, *13*, 3602−3610.

(30) Seo, D. K.; Jeun, J. P.; Kim, H. B.; Kang, P. H. Preparation and characterization of the carbon nanofiber mat produced from electrospun PAN/lignin precursors by electron beam irradiation. *Rev. Adv. Mater. Sci.* **2011**, *28*, 31−34.

(31) Dallmeyer, I.; Lin, L. T.; Li, Y.; Ko, F.; Kadla, J. F. Preparation and characterization of interconnected, kraft lignin-based carbon fibrous materials by electrospinning. *Macromol. Mater. Eng.* **2014**, *299* (5), 540−551.

(32) Xu, X.; Zhou, J.; Jiang, L.; Lubineau, G.; Chen, Y.; Wu, X.; Piere, R. Porous core-shell carbon fibers derived from lignin and cellulose nanofibrils. *Mater. Lett.* **2013**, *109*, 175−178.

(33) Xu, X.; Zhou, J.; Jiang, L.; Lubineau, G.; Payne, S. A.; Gutschmidt, D. Lignin-based carbon fibers: Carbon nanotube decoration and superior thermal stability. *Carbon* **2014**, *80*, 91−102.

(34) Schreiber, M.; Vivekanandhan, S.; Cooke, P.; Mohanty, A.; Misra, M. Electrospun green fibres from lignin and chitosan: A novel polycomplexation process for the production of lignin-based fibres. *J. Mater. Sci.* **2014**, *49* (23), 7949−7958.

(35) Poursorkhabi, V.; Mohanty, A. K.; Misra, M. Electrospinning of aqueous lignin/poly(ethylene oxide) complexes. *J. Appl. Polym. Sci.* **2015**, *132* (2).

(36) Wang, S.; Yang, L.; Stubbs, L. P.; Li, X.; He, C. Lignin-derived fused electrospun carbon fibrous mats as high performance anode materials for lithium ion batteries. *ACS Appl. Mater. Interfaces* **2013**, *5*, 12275−12282.

(37) Schreiber, M.; Vivekanandhan, S.; Mohanty, A.; Misra, M. Iodine treatment of lignin-cellulose acetate electrospun fibres: Enhancement of green fibre carbonization. *ACS Sustainable Chem. Eng.* **2015**, *3* (1), 33−41.

(38) Sattler, R.; Wagner, C.; Eggers, J. Blistering pattern and formation of nanofibers in capillary thinning of polymer solutions. *Phys. Rev. Lett.* **2008**, *100* (16), 164502.

(39) Fong, H.; Chun, I.; Reneker, D. H. Beaded nanofibers formed during electrospinning. *Polymer* **1999**, *40* (16), 4585−4592.

(40) Glasser, W. G.; Jain, R. K. Lignin Derivatives I. Alkanoates. *Holzforschung* **1993**, *47* (3), 225−233.

(41) Kalayci, V. E.; Patra, P. K.; Kim, Y. K.; Ugbolue, S. C.; Warner, S. B. Charge consequences in electrospun polyacrylonitrile (PAN) nanofibers. *Polymer* **2005**, *46* (18), 7191−7200.

(42) Iwamoto, S.; Lee, S. H.; Endo, T. Relationship between aspect ratio and suspension viscosity of wood cellulose nanofibers. *Polym. J.* **2014**, *46* (1), 73−76.

(43) Varesano, A.; Aluigi, A.; Vineis, C.; Tonin, C. Study on the shear viscosity behavior of keratin/PEO blends for nanofibre electrospinning. *J. Polym. Sci., Part B: Polym. Phys.* **2008**, *46* (12), 1193−1201.

(44) Feldman, D.; Banu, D.; Campanelli, J.; Zhu, H. Blends of vinylic copolymer with plasticized lignin: Thermal and mechanical properties. *J. Appl. Polym. Sci.* **2001**, *81* (4), 861−874.

(45) Mousavioun, P.; Halley, P. J.; Doherty, W. O. S. Thermophysical properties and rheology of PHB/lignin blends. *Ind. Crops Prod.* **2013**, *50*, 270−275.

(46) Liu, X.; Xu, Y.; Yu, J.; Li, S.; Wang, J.; Wang, C.; Chu, F. Integration of lignin and acrylic monomers towards grafted copolymers by free radical polymerization. *Int. J. Biol. Macromol.* **2014**, *67*, 483−489.

(47) Coats, A. W.; Redfern, J. P. Kinetic Parameters from Thermogravimetric Data. *Nature* **1964**, *201* (4914), 68−69.

(48) Fernandes, D. M.; Hechenleitner, A. A. W.; Pineda, E. A. G. Kinetic study of the thermal decomposition of poly(vinyl alcohol)/kraft lignin derivative blends. *Thermochim. Acta* **2006**, *441* (1), 101−109.

(49) Corradini, E.; Pineda, E. A. G.; Hechenleitner, A. A. W. Lignin-poly(vinyl alcohol) blends studied by thermal analysis. *Polym. Degrad. Stab.* **1999**, *66* (2), 199−208.

(50) Yang, H.; Yan, R.; Chen, H.; Lee, D. H.; Zheng, C. Characteristics of hemicellulose, cellulose and lignin pyrolysis. *Fuel* **2007**, *86* (12−13), 1781−1788.

(51) Wu, Z.; Wang, S.; Zhao, J.; Chen, L.; Meng, H. Synergistic effect on thermal behavior during co-pyrolysis of lignocellulosic biomass model components blend with bituminous coal. *Bioresour. Technol.* **2014**, *169*, 220−228.

(52) Guo, Z.; Bai, Z.; Bai, J.; Wang, Z.; Li, W. Synergistic effects during co-pyrolysis and liquefaction of biomass and lignite under syngas. *J. Therm. Anal. Calorim.* **2015**, *119*, 2133−2140.

(53) Lisperguer, J.; Perez, P.; Urizar, S. Structure and thermal properties of lignins: Characterization by infrared spectroscopy and differential scanning calorimetry. *J. Chil. Chem. Soc.* **2009**, *54* (4), 460−463.

(54) Tejado, A.; Peña, C.; Labidi, J.; Echeverria, J. M.; Mondragon, I. Physico-chemical characterization of lignins from different sources for use in phenol−formaldehyde resin synthesis. *Bioresour. Technol.* **2007**, *98* (8), 1655−1663.

(55) Lee, S.; Kim, J.; Ku, B. C.; Kim, J.; Joh, H. I. Structural evolution of polyacrylonitrile fibers in stabilization and carbonization. *Adv. Chem. Eng. Sci.* **2012**, *2*, 275−282.